Contribution from the Department of Chemistry, University of the Western Cape, Bellville 7530, South Africa, and Laboratorium für Chemische und Mineralogische Kristallographie, Universität Bern, Freiestrasse 3, CH-3012 Bern, Switzerland

Molecular Geometry of d^8 Five-Coordination. 3. Factor Analysis, Static Deformations, and Reaction Coordinates

Thomas P. E. Auf der Heyde*,† and Hans-Beat Bürgi‡

Received December 2, 1988

The molecular geometry of ML_5 fragments has been shown to be characterized essentially by three archetypal conformations: a trigonal bipyramid (TBP) of D_{3h} symmetry, and a "flattened" square pyramid (fSQP) and an "elevated" square pyramid (fSQP), both of C_{4v} symmetry. This paper, the last of a three-part series, employs the technique of factor analysis in order to map the characteristic distortions of these three archetypal conformations. In all cases, their static deformations mirror distortions expected along particular chemical reaction coordinates. The TBP is shown to map a classical S_N2 coordinate, a Berry intramolecular exchange coordinate, and a coordinate indicating the preservation of a constant amount of bonding at the central metal atom, the "glue" coordinate. Both the eSQP and fSQP distort along the glue coordinate and along a coordinate delineating the pyramidalization of the pyramid. The sum of these is akin to a coordinate mapping the reversible addition of a fifth ligand to a square-planar ML_4 center. Furthermore, the eSQP also distorts according to the Berry coordinate, while the fSQP interestingly does not. Parallels are outlined between these static deformations and the solution dynamics of five-coordinate species, and these are discussed in the light of the structure correlation hypothesis.

Introduction

In part 2 of this study,[1] we analyzed the distribution of observed molecular structures of five-coordinate d^8 metal complexes in terms of the distribution of their representative points in 12-dimensional spaces. These spaces are defined by 12 nonredundant symmetry coordinates representing the idealized trigonal bipyramid (TBP) of D_{3h} symmetry (T-space), and those representing the idealized square-based pyramid (SQP) of C_{4v} symmetry (S-space), respectively. We found that the molecular geometries were grouped essentially into two conformations in T-space: a slightly distorted TBP of D_{3h} symmetry characterized by the cluster we called T3 and a "SQP" of C_{2v} symmetry (dSQP) characterized by cluster T1. In S-space, however, three archetypal conformations were revealed: a slightly distorted C_{2v} "TBP" (dTBP, cluster S1), a "flattened SQP" (fSQP, cluster S2), and an "elevated SQP" (eSQP, cluster S4), the latter two with a perfect C_{4v} symmetry.

The analysis of the correlation matrices for T-space, T1 and T3, revealed that three major distortions characterized the data distribution. These were described in terms of adherence to an S_N2 coordinate,[2] a Berry coordinate, and a glue coordinate,[3] with the S_N2 distortion associated with cluster T3 (TBP) and the glue distortion with cluster T1 (dSQP), and the Berry coordinate being manifested in both clusters. In the case of S-space, univariate and bivariate statistics suggest that the variance lies primarily along a coordinate mirroring a reversible addition/elimination reaction at a square-planar center. Apparently two types of distortion together give rise to this coordinate; when the glue coordinate[4] is correlated to the flattening or elevation of the SQP, the addition/elimination coordinate arises. Some variance also appears to be associated with the Berry coordinate. This distortion is mapped by clusters S1 (dTBP) and S4 (eSQP) but not, however, by S2 (fSQP), while the addition/elimination coordinate is associated with S2 and S4. Cluster S1 also appears to distort along an S_N2 coordinate.

Cluster analysis has established the broad outlines of the data distribution; factor analysis will now be used in order to explore the shape of these distributions, i.e. to map more rigorously the coordinates along which the clouds of data points expand. This will yield a picture of the generalized distortions that the ML_5 molecular fragment manifests in the solid state. In a previous paper,[5a] we have attempted to present a simplified outline of the application of factor analysis to a generalized chemical data set. We shall therefore simply point out here that factor analysis extracts linear combinations of the original variables, which describe, in turn, the greatest amount of sample variance, the second greatest, and so on, from an *eigenanalysis* of the covariance or correlation matrix.[5b,c]

Murray-Rust, in particular, has pioneered the application of this technique to the analysis of molecular structure.[6-8] He has shown[8] how the mathematical treatment of normal-coordinate analysis closely parallels that of factor analysis. This arises from the possibility of factorizing, in the same way, both the matrix of force constants that appears in the potential energy expression of the general valence force field and the matrix of the covariances or correlations between the symmetry coordinates which forms the basis of the factor analysis. As a consequence of this parallel, the most important factors will be closely related to normal coordinates with low force constants. He has pointed out, however, that this parallel can easily be destroyed by rotation of the factor axes, if rotation does not occur *within* blocks of the matrix, since the rotated factors no longer lie along the eigenvectors (the directions of maximum variance). Factor rotation therefore has to be treated cautiously, and we shall consequently only include rotation where it has helped the interpretation, or *reification*, of the factors.[9] During the factor analysis we shall pay particular attention to the *symmetry* of the results, since these should reflect the symmetry inherent in the data distribution as a consequence of the replication of individual representative points into their isometric partners in the parameter space.[1]

Experimental Section and Results

1. Setting the Parameters. P4M, the BMDP[1] factor analysis program, can extract factors from either the covariance or the correlation matrix by a number of different methods including

* To whom correspondence should be addressed
† University of the Western Cape.
‡ Universität Bern.

(1) See: Auf der Heyde, T. P. E.; Bürgi, H.-B. *Inorg. Chem.*, preceding paper in this issue.
(2) When it is restricted to small deviations from D_{3h} symmetry, this distortion could also be considered as an axial trans-influence coordinate.
(3) Restricted to small deviations from D_{3h} symmetry, it could also be called an axial–equatorial cis-influence coordinate.
(4) Apical–equatorial cis-influence coordinate.
(5) (a) Auf der Heyde, T. P. E. Submitted for publication in *J. Chem. Educ.* (b) Malinowski, E. R.; Howery, D. G. *Factor Analysis in Chemistry*; John Wiley and Sons: New York, 1980. (c) In this and the previous papers we follow the BMDP manual (see ref 6 in preceding paper) in our use of the term "factor analysis". It has been argued that the term "principal component analysis" might be more appropriate for the technique used here. See: Chatfield, C.; Collins, A. J. *Introduction to Multivariate Analysis*; Chapman and Hall: London, 1980.
(6) Murray-Rust, P.; Motherwell, S. *Acta Crystallogr.* **1983**, *B39*, 2534-2546.
(7) Domenicano, A.; Murray-Rust, P.; Vaciago, A. *Acta Crystallogr.* **1983**, *B39*, 457-468.
(8) Murray-Rust, P. *Acta Crystallogr.* **1982**, *B38*, 2765-2771.
(9) As it turns out, there are only two cases where rotation gives chemically more intelligible results than do the unrotated factors.

0020-1669/89/1328-3982$01.50/0

Table I. Results of Factor Analysis of T-Space[a]

cluster	factors	sym	% var[b]	coord
T-space	F1 = $0.743S_{5a} + 0.935S_{6a} + 0.554S_{7a}$	E′	18	Berry
	F2 = $0.743S_{5b} + 0.935S_{6b} + 0.554S_{7b}$	E′	18	Berry
	F3 = $-0.914S_3 + 0.914S_4$	A_2''	14	S_N2
	F4 = $-0.880S_1 + 0.880S_2$	A_1''	13	glue
	F5 = $-0.605S_{5b} + 0.804S_{7b}$	E′	9	
	F6 = $-0.605S_{5a} + 0.804S_{7a}$	E′	9	
T1 (dSQP)	F1 = $-0.838S_1 + 0.866S_2 + 0.940S_{5a} + 0.680S_{6a} - 0.605S_{7a}$	$A_1' + E'$	26	add/el
	F2 = $-0.530S_3 + 0.801S_4 + 0.670S_{8a}$	$A_2'' + E''$	12	angular flexibility
	F3 = $-0.730S_{5b} + 0.359S_{6b} + 0.796S_{7b}$	E′	11	angular flexibility
T3 (TBP)	F1 = $-0.959S_3 + 0.959S_4$	A_2''	15	S_N2
	F2 = $0.358S_{5b} + 0.877S_{6b} + 0.707S_{7b}$	E′	12	Berry
	F3 = $0.358S_{5a} + 0.877S_{6a} + 0.707S_{7a}$	E′	12	Berry
	F4 = $0.793S_1 - 0.793S_2$	A_1'	10	glue
	F5 = $0.874S_{5a} + 0.105S_{6a} - 0.573S_{7a}$	E′	9	
	F6 = $0.874S_{5b} + 0.105S_{6b} - 0.573S_{7b}$	E′	9	

[a] Only unrotated factors with eigenvalues greater than unity are shown. Key: sym = symmetry of factor; % var = percentage of sample variance explained by each factor; coord = general distortion mapped by the factor; add/el = addition/elimination. [b] Although the term % var (percent variance) is used here, it should be remembered that the factor analysis was performed on the correlation matrix and not on the covariance matrix.

principal components. Several methods of rotation are available, including orthogonal and oblique rotation, and the number of factors, the number of iterations, and the cutoff points can be chosen by the user. The output contains, among others, univariate and bivariate statistics, eigenvalues and corresponding factor loadings, percentage of variance accounted for by the factor, rotated factor loadings, and scatterplots of these.

In all cases, we chose the correlation matrix as the matrix to be factored, with the method for initial factor extraction as principal component analysis.[5c] Only factors whose eigenvalues exceeded unity (Kaiser's criterion) were retained, and rotation was orthogonal.

2. T-Space. Results of the factor analysis are listed in Table I, while Figure 1 graphically illustrates the corresponding distortion coordinates. The symmetry of the data distribution manifests itself in both the relation *between* factors representing the two partners of a degenerate representation (e.g. F1 and F2 for T-space overall—they are both of E′ symmetry[10]), as well as in the relation between symmetry equivalent parameters *within* a factor, which have identical absolute loadings (e.g. symmetry coordinates S_3 and S_4 in F3 of T-space overall—both belong to the A_2'' representation). In other words, the requirement that the symmetry inherent in the data distribution manifest itself in the results of factor analysis (as it did earlier in those of cluster analysis[1]) has been met.

(a) T-Space Overall. For T-space overall, the most important coordinate mapped is the Berry intramolecular exchange coordinate. This is characterized by the degenerate factor F1 and F2, which accounts for 28% of the sample variance. The second most important coordinate is the S_N2 coordinate mapped by F3, which is of A_2'' symmetry and accounts for 14% of the variance, while the constant-amount-of-glue coordinate appears in F4 (A_1' symmetry, 13% of variance). The degenerate factor F5 plus F6, of E′ symmetry and accounting for 18% of variance, is interesting in that it maps a distortion that can be interpreted in two ways. These are related to whether this distortion is primarily associated with the TBP cluster (T3) or with the SQP cluster (T1). In the event of the former, we can argue that this distortion resembles the incipient stages of the Berry intramolecular exchange coordinate, whereas in the latter it might be more appropriate to describe it as mirroring the incipient stages of a reversible addition/elimination reaction at a square-planar center.

(b) T1. Cluster T1 (dSQP), in contrast to T3 (TBP) and T-space overall, exhibits mixing of coordinates from different symmetry species in the same factor. This clearly is related to the inability of this cluster to conform to the symmetry of parameter space.[1] Figure 1 graphically illustrates the distortions mapped by the factors, but superimposed this time onto a SQP framework in order to facilitate the reification of the factors. F1 rather obviously resembles the expected distortions occurring during a reversible addition/elimination reaction at a square-planar center, and it conforms to C_{2v} symmetry. F2 and F3 can be interpreted as a manifestation of an easily deformable SQP molecular fragment, a fragment exhibiting a large degree of angular flexibility (see discussion of S-space below). It is important, though, that both factors preserve elements of C_{2v} symmetry as well; they preserve the $\sigma_v(xz)$ and $\sigma'_v(yz)$ elements, respectively.

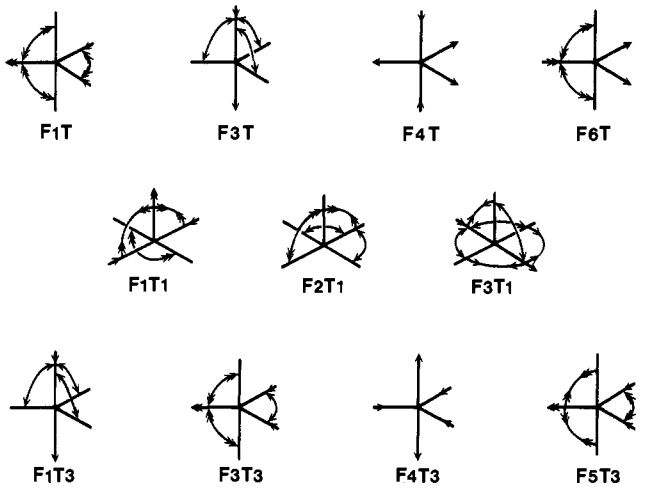

Figure 1. Graphic representation of factors describing T-space overall (F*n*T; n = 1, 3, 4, 6), cluster T1 (F*n*T1; n = 1–3), and cluster T3 (F*n*T3; n = 1, 2, 4, 5). Diagrams are constructed by superimposing the distortion due to each of the symmetry coordinates that are components of a factor onto *one* framework. Only *independent distortions* are indicated for the sake of visual simplicity. The number of heads to the arrows is a consequence of the superposition of symmetry coordinates and it not related to their loading in a factor. The SQP framework was chosen for cluster T1 since its archetype is a dSQP. F2T, F5T, F2T3, and F6T3 are not illustrated since they simply form partners to F1T, F6T, F2T3, and F6T3 in the corresponding degenerate irreducible representation, and their inclusion would not simplify the interpretation.

(c) T3. The variance in T3 (TBP) is associated with the S_N2 distortion coordinate (F1, A_2'' symmetry, 15% of variance), the Berry coordinate (F2 plus F3, E′ symmetry, 24% of variance) and the glue coordinate (F4, A_1' symmetry, 10% of variance). These distortions are all diagrammatically represented in Figure 1, as is F5. This factor features the same components (S_{5a}, S_{6a}, S_{7a}) as the Berry factor (F3), except that the loading for S_{7a} in F5 is negative, while it is positive in F3 and all other Berry coordinates. The opening up of an equatorial angle concomitant with a shortening of the two bonds containing it can be explained on the basis of simple steric requirements. The negative correlation of

(10) Such factors will henceforth be termed degenerate factors.

Table II. Relative Importance of Bond Symmetry Coordinates (S_1, S_2, S_3, S_{5a}, S_{5b}) (Å) and Angular Coordinates (S_4, $S_6 - S_8$) (Å) in the Factors for T-Space (T) and Clusters T1 and T3

	S_1	S_2	S_3	S_4	S_{5a}	S_{5b}	S_{6a}	S_{6b}	S_{7a}	S_{7b}	S_{8a}	S_{8b}
F1T					0.189		1.156		0.129			
F2T						0.189		1.156		0.129		
F3T			−0.121	0.327								
F4T	−0.150	0.118										
F5T						−0.154				0.187		
F6T					−0.154				0.187			
F1T1	−0.125	0.121			0.327		0.294		−0.142			
F2T1			−0.036	0.197							0.212	
F3T1						−0.060		0.158		0.156		
F1T3			−0.210	0.512								
F2T3						0.029		0.291		0.124		
F3T3					0.029		0.291		0.124			
F4T3	0.151	−0.067										
F5T3					0.072		0.035		−0.100			
F6T3						0.072		0.035		−0.100		

S_{7a} (the widening of the already large axial angle) with S_{5a} and S_{6a} might result from steric crowding brought about by the opening of the equatorial bond.

(d) Relative Importance of Symmetry Coordinates. The graphic representation of distortions mapped by the factors is useful in their reification and translation into chemical terms, but it attaches equal absolute importance to each symmetry coordinate in a factor. The loadings of the coordinates can give some idea of the significance of a particular distortion, but the relative importance of the symmetry coordinates must be established by multiplying their standard deviations by their loading in a given factor. Table II reports the relative importance of each symmetry coordinate in the factors extracted for T-space overall and for clusters T1 (dSQP) and T3 (TBP). It affords slightly more insight into the details of the distortions mapped by some of the factors. For example, F1 for T-space, which maps the Berry coordinate, seems to be dominated by S_{6a}, the opening of the equatorial angle (θ_{24}) that accompanies the intramolecular exchange. A chemical interpretation of this might be that the relative change that this angle has to undergo along the Berry coordinate is greater than that experienced by the axial angle (θ_{15}). This would conform to the results of cluster analysis, which indicate that an "average" SQP—which would presumably approximate to that on the Berry coordinate—has trans-basal angles $\theta_{15} = \theta_{24} = 166°$, implying that θ_{24} needs to change by 46° but θ_{15} only by 14°. Apart from F1, no other factor seems to contain symmetry coordinates whose importance is either vastly greater or smaller than that of the others in that factor.

For F2 in Cluster T1 (dSQP), symmetry coordinate S_3, mapping the simultaneous lengthening and shortening of a pair of trans-basal bonds, appears to be much less significant than S_4 or S_{8a}, both of which reflect the angular flexibility referred to earlier. How much of this different is due to the comparison of different kinds of symmetry coordinates (incremental versus angular) and how much of it might reflect real differences in the degree of distortion is difficult to judge. For T3 (TBP), the most striking difference in relative importance is that between S_{5a} and both S_{6a} and S_{7a} in F3, the Berry factor. The data suggest that changes in the equatorial bond lengths—the pivotal bond becomes longer, the other two shorter—are far less important along the Berry coordinate than are the changes in angles (specifically the equatorial angle, θ_{24}, and the axial angle, θ_{15}). In other words, a given molecular conformation could easily be distorted along the C_{2v} exchange coordinate in terms of adjustments of its angles, without its bond lengths necessarily having to conform rigidly to the requirement that the pivotal (soon to be apical) bond be much longer than the basal ones. This, of course, also conforms to chemical criteria, since we know that a range of SQPs with differing apical bond lengths exist and that, in any case, this bond can adapt to any length without affecting the C_{2v} symmetry anywhere along the Berry coordinate. How much of the difference in the relative importance of S_{5a} and the pair S_{6a},S_{7a} is the result, again, of comparing bond symmetry coordinates with angular ones and how much of it reflects real structural factors are difficult to assess, though.[11]

Table III. Results of Factor Analysis of T-Space Excluding All Nickel Compounds[a]

factor	sym	% var[b]	coord
F1 = $-0.956S_1 + 0.956S_2$	A′	18	glue
F2 = $0.739S_{5a} + 0.921S_{6a} + 0.397S_{7a}$	E′	13	Berry
F3 = $0.739S_{5b} + 0.921S_{6b} + 0.397S_{7b}$	E′	13	Berry
F4 = $-0.830S_3 + 0.830S_4$	A_2''	11	S_N2
F5 = $-0.586S_{5a} + 0.091S_{6a} + 0.880S_{7a}$	E′	9	
F6 = $-0.586S_{5b} + 0.091S_{6b} + 0.880S_{7b}$	E′	9	
F7 = $1.00S_{8a}$	E″	8	
F8 = $1.00S_{8b}$	E″	8	

[a] Key: sym = symmetry of factor; % var = percentage of variance explained by the factor; coord = general distortion mapped by the factor. Only factors with eigenvalues greater than unity are listed. [b] See footnote *b* of Table I.

(e) T-Space minus Nickel Compounds. Since nickel compounds represent the largest homogeneous grouping in the data (113 out of 196 entries) it is of interest to establish whether the results of the analysis are in any way dominated by this grouping, in which case this would point to an inherent difference between five-coordination in nickel and that in the other metals. Table III illustrates the results of factor analysis of T-space *excluding* nickel entries.

The order of importance of the coordinates has altered somewhat from that of T-space including nickel (Table I). Essentially, the glue coordinate becomes slightly more important and the S_N2 slightly less important on exclusion of nickel. This correlates well with the facts established earlier. First, the glue coordinate seems to be more closely associated with the square pyramidally disposed structure, being an important component in the addition/elimination coordinate for a square-planar center—the change in bond lengths, in particular that of the apical bond, is more important in this coordinate and the fSQP → eSQP distortion than it is for the S_N2 coordinate at a TBP. Second, by far the majority of TBP compounds are nickel-containing (45 out of 59). Exclusion of the nickel entries would therefore increase the relative amount of the SQP structures in T-space, and consequently result in magnifying all those factors primarily associated with this conformation. It is interesting to note that the remaining 14 TBP conformations still make mapping of the S_N2 coordinate possible.

The relatively unaltered importance of the Berry coordinate as the primary distortion in T-space does not come as a surprise in view of the ability of both the TBP and the SQP conformations to manifest such C_{2v} distortions. In this light is is surprising,

(11) One way of doing this, perhaps, could be the calculation of the relative importance of each internal coordinate by multiplication of the inverse symmetry coordinate matrix with the relative importance of the symmetry coordinates in each factor. This would still require, though, a comparison of bond distance increments and angles, albeit scaled angular displacements.

Table IV. Results of Factor Analysis of S-Space[a]

cluster	factors	sym	% var[b]	coord
S-space overall	$F1' = 0.917S_1 - 0.888S_2 + 0.765S_3$	A_1	14	add/el
	$F2' = 0.863S_{7a} - 0.516S_{8a} - 0.562S_{9a} - 0.562S_{9b}$	E	14	S_N2
	$F3' = 0.863S_{7b} - 0.516S_{8b} + 0.562S_{9a} - 0.562S_{9b}$	E	14	S_N2
	$F4' = 0.832S_4 + 0.832S_5$	B_1	12	Berry
	$F5' = 1.000S_6$	B_2	9	
S1 (dTBP)	$F1 = -0.914S_{7a} + 0.853S_{8a} + 0.888S_{9a} + 0.888S_{9b}$	E	26	S_N2
	$F2 = -0.439S_1 + 0.770S_2 - 0.651S_3 + 0.781S_4 + 0.731S_5$	$A_1 + B_1$	20	
	$F3 = 0.821S_{7b} - 0.817S_{8b}$	E	11	
	$F4 = -0.542S_1 + 0.349S_2 + 0.610S_3 + 0.284S_4 - 0.454S_5$	$A_1 + B_1$	9	
S2 (fSQP)	$F1 = 0.917S_1 - 0.842S_2 + 0.292S_3$	A_1	14	add/el
	$F2 = 0.822S_4 - 0.822S_5$	B_1	11	
	$F3 = 0.546S_{7a} + 0.546S_{7b} - 0.556S_{8a} - 0.556S_{8b} + 0.297S_{9b}$	E	11	angular flexibility
	$F4 = 0.546S_{7a} - 0.546S_{7b} - 0.556S_{8a} + 0.556S_{8b} + 0.297S_{9a}$	E	11	angular flexibility
	$F5 = 0.064S_1 + 0.396S_2 + 0.939S_3$	A_1	9	elevation of SQP
S4 (eSQP)	$F1' = 0.888S_1 - 0.879S_2 + 0.291S_3$	A_1	14	add/el
	$F2' = 0.837S_4 + 0.837S_5$	B_1	12	Berry
	$F3' = 0.740S_{7a} + 0.516S_{8a} - 0.541S_{9a} - 0.541S_{9b}$	E	12	angular flexibility
	$F4' = 0.740S_{7b} + 0.516S_{8b} + 0.541S_{9a} - 0.541S_{9b}$	E	12	angular flexibility
	$F5' = 1.000S_6$	B_2	9	

[a] Primed factors are rotated; unprimed factors are unrotated. Only factors whose eigenvalues are greater than unity are listed. In each factor, only those symmetry coordinates whose relative importance is greater than 0.01 Å are tabulated. Key: sym = symmetry of factor; % var = percentage variance explained by each factor; coord = general distortion mapped by the factor; add/el = addition/elimination. [b] See footnote *b* of Table I.

though, that the Berry coordinate (as mapped by S_{5a}, S_{6a}, and S_{7a} in T-space) is not manifest in the T1 (dSQP) cluster. Perhaps this is related to the clusters' inability to conform fully to the symmetry of T-space.

F5 and F6 show the same inverse relation of S_{5a} to S_{6a} and S_{7b} (or, respectively, S_{5b}, S_{6b}, and S_{7b}) as was observed earlier for F5T3 and F6T3; their loadings are of opposite sign, whereas in the Berry factors (F1T, F2T, F2T3, and F3T3) they are all of the same sign. What is more, is that this curious distortion is still as important *after* the exclusion of nickel entries as it is *prior* to. This would suggest that the distortion is related mainly to the remaining compounds, i.e. that it results from some distortion of the SQP conformation that happens to be mapped by this factor.

3. S-Space. Table IV illustrates the results of factor analysis of S-space, while Figure 2 represents graphic illustrations of the factors. The symmetry of the data distribution reemerges in the symmetry of the factors. For S2, S4, and S-space overall the factors do not mix symmetry coordinates from different irreducible representations, and the two partners of a degenerate factor have identical eigenvalues (and, hence, percentage variance), with the absolute loadings of identical symmetry coordinates in the two partners being equal. S1 mixes the species as did T1 in the case of T-space. Most likely this is also a consequence of this cluster's inability to conform fully to C_{4v} symmetry, exhibiting only C_{2v} symmetry instead.

(a) S-Space Overall. The most dominant distortion mapped seems to be the S_N2 coordinate for a trigonal bipyramidally disposed conformation. This coordinate manifests itself in the degenerate factor whose two partners are F2′ and F3′, and it accounts for 28% of variance. The next important one is the addition/elimination coordinate mapped by F1′, accounting for 18% of sample variance. F4′ maps the Berry coordinate describing 12% of sample variance. The last factor F5′ (whose eigenvalue is greater than unity) does not correspond to any recognizable chemical coordinate but gives the distinct impression that it could be related to the presence of a group of compounds containing either two rather rigid bidentate ligands with small bites or a macrocycle of some kind.

In this case, the unrotated factors F2 and F3 (% Var = 14) contained two symmetry coordinates (S_{7a}, S_{8a} and S_{7b}, S_{8b}, respectively) whose loadings were small, but not quite zero, resulting in distortions that could not be sensibly interpreted. Rotation of the factor axes left F1, F4, and F5 unchanged but considerably simplified the reification of F2′ and F3′.

(b) S1. Not unexpectedly this cluster is characterized by the S_N2 coordinate, mapped by F1 of E symmetry and accounting for 26% of sample variance. The expected partner to F1 under the E representation is not immediately obvious, and the only possibility seems to be F3, which contains two of the four expected symmetry coordinates and accounts for 11% of variance. The last factor, a mixture of A_1 and B_1 representations, essentially maps the opening of an equatorial angle in the TBP with a concomitant shortening of the bond opposite this angle and a lengthening of the axial bonds. The related coordinate, F2, differs in that while the axial bonds lengthen, the equatorial angle decreases. Alternatively, the positive correlation between S_4 and S_5 in this factor can be interpreted as mapping the Berry coordinate, while the factor's other components (S_1, S_2, S_3) trace the addition/elimination or glue coordinate. In this sense, then, the results obtained for T3 (TBP) and those of S1 (dTBP) would correspond: in the former, the factors are (i) S_N2, (ii) Berry, and (iii) glue, while the S_N2 coordinate and a combination of Berry and glue distortions constitute the factors for S1. There seems no clear chemical description of the distortions mapped by F3 and F4. Arguably,

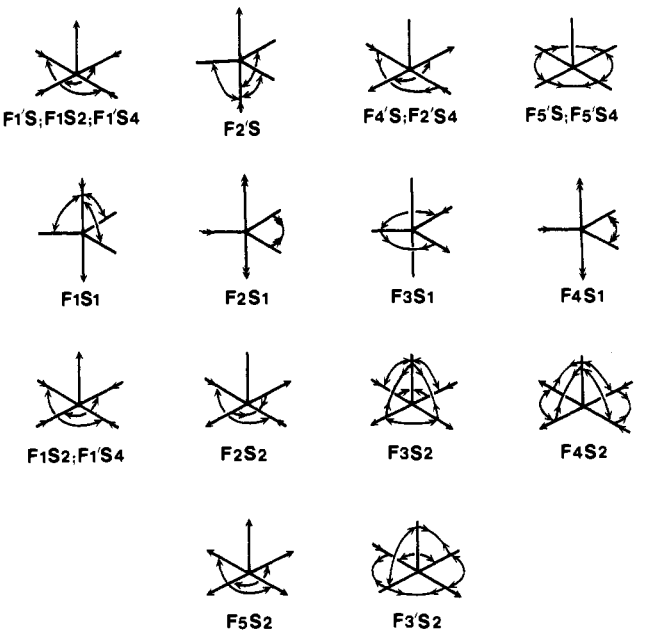

Figure 2. Graphic representation of factors describing S-space overall (F*n*S; *n* = 1′, 2′, 4′, 5′), cluster F1 (F*n*S1; *n* = 1–4), cluster S2 (F*n*S2; *n* = 1′, 2′, 3′, 5′) and cluster S4 (F*n*S4; *n* = 1′, 2′, 3′, 5′). Only those independent distortions are shown whose relative importance in the factor exceeds 0.01 Å. F2′S is shown with reference to a TBP in order to facilitate its reification.

Table V. Relative Importance of Bond Symmetry Coordinates (S_1, S_2, S_4, S_{7a}, S_{7b}) (Å) and Angular Coordinates (S_3, S_5, S_6, S_8, S_9) (Å) in the Factors for S-Space (S) and Clusters S1, S2, and S4[a]

	S_1	S_2	S_3	S_4	S_5	S_6	S_{7a}	S_{7b}	S_{8a}	S_{8b}	S_{9a}	S_{9b}
F1′S	0.291	−0.157	0.376									
F2′S							0.095		−0.186		−0.142	−0.142
F3′S								0.095		0.186	0.142	−0.142
F4′S				0.091	0.667							
F5′S						0.268						
F1S1							−0.186		0.294		0.276	0.276
F2S1	−0.038	0.103	−0.161	0.115	0.232							
F3S1								0.070		−0.250		
F4S1	−0.047	0.047	0.151	0.042	−0.144							
F1S2	0.274	−0.098	0.063									
F2S2				0.045	−0.171							
F3S2							0.039	0.039	−0.272	−0.272		0.061
F4S2							0.039	−0.039	−0.272	0.272		0.061
F5S2	0.019	0.046	0.202									
F1′S4	0.111	−0.103	0.086									
F2′S4				0.065	0.233							
F3′S4							0.055		0.165		−0.119	−0.119
F4′S4								0.055		0.165	0.119	−0.119
F5′S4						0.260						

[a] Rotated factors are denoted by primes.

F3 may reflect an equatorial cis influence, but most likely their complexity is not unrelated to the imcompatibility of the symmetry of this cluster to that of S-space.

(c) S2. F1 here combines the glue coordinate (S_1 and S_2) with the flattening/elevation of the SQP (S_3) to map the addition/elimination coordinate. It is of A_1 symmetry and explaines 14% of sample variance. The degenerate factor with components F3 and F4, accounting for 22% of variance, seems to map the angular flexibility that was referred to previously, whereby the position of the apical ligand relative to the ML_4 fragment (the metal with four basal ligands) is rather variable in terms of both its distance to the metal and the angles between it and the ML_4 fragment. F5 (A_1 symmetry, 9% of variance) contains the same components as F1 (addition/elimination), but their loadings are of different sign. Consequently, it appears that this factor simply maps the flattening/elevation of the fSQP (S_2), since the distortion in the bond lengths (S_1, S_2) is not correlated as it should be for the addition/elimination coordinate. Finally, F2 is curious in that it contains the Berry coordinate components (S_4 and S_5), but they are negatively correlated, instead of positively, which they would be if mapping the intramolecular exchange coordinate. The most likely explanation is that this factor simply maps the response—under the constraint of C_{4v} symmetry—of the fSQP to a shortening or lengthening of its basal bonds and that it is unrelated to the Berry coordinate, which is manifested only by the eSQP. It might also be taken as implying that the fSQP does not undergo Berry rotation or is not an intermediate on the Berry coordinate.

(d) S4. This cluster also has 14% of its variance associated with the addition/elimination coordinate that is mapped by F1′, as was the case for S2. The Berry coordinate, which was identified by F4′ for S-space overall but not picked up in S1 (dTBP), is mapped by F2′, and it accounts for 12% of sample variance. The degenerate factor represented by F3′ and F4′, describing 24% of variance, contains components similar to those of F3S2 and F4S2, suggesting that it also mirrors the flexibility in the apical bond with respect to the residual ML_4 fragment. Finally, F5′ clearly is identical with F5S, the factor that possibly reflects the presence of a group of compounds with severely constraining ligands, either two bidentate ligands with small bites or a macrocycle.

In this case, rotation was essentially employed in order to simplify F2, which contained four components with loadings below 0.09 while two components had loadings on the order of 0.8. On rotation, the small loadings disappeared and the interpretation of F2′ was vastly simpler. F1 and F5 remained unchanged, while the previous slight asymmetry in the factor loadings of F3 and F4 was removed upon rotation.

In summary, the results obtained for T1 (dSQP) and those for S2 (fSQP) and S4 (eSQP) correlate well. In the former the addition/elimination and the angular flexibility coordinate only were identified, while for the SQP clusters in S-space these two distortions were mapped, with the addition of the Berry coordinate in the case of S4 (eSQP). Quite possibly the absence of the Berry coordinate in T1, already commented upon earlier, is also related to the mixing of S2 (fSQP) and S4 (eSQP) in T1 (dSQP), with distortions manifested only by S4 being eclipsed on the merging of these two clusters. This phenomenon, most likely, is enhanced by the fact that in T-space only *half* the possible variance in the SQP conformations is manifested, effectively, since the *full* C_{4v} symmetry of this variation cannot emerge due to the constraints placed upon it by the symmetry of the D_{3h} data space.

(e) Relative Importance of Symmetry Coordinates. There appear to be no significant differences in the relative importances of the various symmetry coordinates as collected in Table V in the factors extracted for S-space overall. What small differences there are, could well result from the comparison of bond and angular symmetry coordinates (e.g. S_{7a} and S_{8b} in F2′S), with the possible exception of F4′. This factor reflects the Berry coordinate, S_4 mapping the lengthening of (soon to become) axial bonds and the shortening of equatorial ones, while S_5 maps the opening and closing of the respective trans-basal angles, which is concomitant with the changes in bond lengths. From the relative importances listed in Table V, it might be argued that the change in bond lengths accompanying a distortion along the Berry coordinate is considerably less important than the angular changes occurring during this distortion. This conclusion tallies well with that made from an analysis of F1 for T-space in which the angular coordinate mapping the opening of the equatorial angle (S_{6a}) was also considerably more important than that describing the simultaneous bond length changes. For S1 all of F2, F3, and F4 manifest small differences in importance among the various symmetry coordinates. Quite possibly, though, these differences spring from the same problem that, in the first place, is responsible for the emergence of these complex factors which map no chemically meaningful distortion—that of the incompatibility of S1 with the symmetry of S-space.

The flexibility in the position of the apical ligand appears to be of primary importance in accounting for the variability among the fSQPs (S2). In F1 the distance of this ligand from the metal (S_1) is rather more important than that of the others (S_2) and than the variability in the trans-basal angles (S_3). This suggests that the approach of the apical ligand to the residual ML4 fragment along the addition/elimination coordinate is, at least initially, not accompanied by much elevation in the fSQP. In F3 and F4 the angular flexibility of the apical ligand (S_{8a}, S_{8b}) dominates slightly, suggesting that the angle of approach (or departure) of the apical ligand is not limited strictly to the per-

Table VI. Results of Factor Analysis of S-Space Excluding All Nickel Compounds[a]

factor	sym	% var[b]	coord
$F1 = 0.962S_1 - 0.935S_2 + 0.614S_3$	A_1	18	add/el
$F2 = 0.828S_{7b} - 0.247S_{8b} + 0.516S_{9a} - 0.516S_{9b}$	E	11	S_N2
$F2' = 0.800S_4 + 0.800S_5$	B_1		Berry
$F3 = 0.828S_{7a} - 0.247S_{8a} - 0.516S_{9a} - 0.516S_{9b}$	E	11	S_N2
$F3' = -0.500S_{7a} - 0.500S_{7b} + 0.855S_{9b}$	E		
$F4 = 0.799S_4 + 0.799S_5$	B_1	11	Berry
$F4' = -0.500S_{7a} + 0.500S_{7b} + 0.855S_{9a}$	E		

[a] Rotated factors are denoted by primes. Key: sym = symmetry of factor; % var = percentage of variance accounted for by factor; coord = general distortion mapped by the factor; add/el = addition/elimination. Only the first four factors have been listed, and only compounds with loadings greater than 0.1 are included in the factors. [b] See footnote *b* of Table I.

pendicular line through the center of the basal L_4 plane of the SQP. In F5 (the "elevation" coordinate) the variability in the trans-basal angles (S_3) seem to be most important, while bond distances (S_1, S_2) play a much less significant role. This suggests, as does F1, that there is a degree to which the pyramidalization at the metal is independent of the proximity of the apical ligand.

For the addition/elimination coordinate (F1′) in S4 (eSQP), however, the proximity of all five ligands to the metal and the degree of pyramidalization appear to be more closely linked than in the fSQP, as indicated by the very similar relative importances of the bond distances (S_1, S_2) and angles (S_3) in this factor. This might suggest that as the addition of the apical ligand proceeds, a point is reached at which the elevation of the metal from the basal L_4 plane is at a maximum, although the apical bond has not yet shortened to its minimum. At this juncture, the relative importances switch over from what they are in S2 (fSQP), and changes in bond distances predominate over those in the degree of pyramidalization. Alternatively, if one assumes the eSQP to be representative of the end of the addition/elimination coordinate, then the important role which this factor has in accounting for the variance in S4 (14%) would suggest that the Berry and the addition/elimination coordinate might well be adhered to simultaneously. Purely from symmetry considerations this would seem unlikely, though, since the symmetries of the two distortions are different—the addition/elimination coordinate is of A_1 symmetry, while the Berry is of B_1 symmetry. For the Berry coordinate F2′ in S4 the bond distances (S_4) again seem less significant in describing the variance along this distortion than the trans-basal (or, soon to be, axial and equatorial) bonds (S_5) seem to be.

Overall, the reification of the factors extracted for S-space and its clusters has been rather more difficult than it was in the case of T-space. This is manifested, first, in the need for factor rotation and, second, in the considerably more complex nature of the distortions mapped by the factors. Quite likely this stems from the closer proximity and greater diffusion of the clusters in S-space;[1] a complication arises in the extraction of "pure" factors from clouds of representative points when the distributions merge or overlap.

(f) S-Space minus Nickel Compounds. The results of factor analysis on the S-space data excluding nickel compounds are tabulated in Table VI. Where they differ, both rotated and unrotated factors are shown. Prior to rotation, the order of the factors was (i) S_N2 (22% of variance), (ii) addition/elimination (18%), and (iii) Berry (11%). After rotation, it altered to (i) addition/elimination (18%), and (ii) Berry (11%), with the S_N2 coordinate all but disappearing. Both these results ought to be compared to the results for S-space including nickel entries, where the order in factors is (i) S_N2 (28%), (ii) addition/elimination (14%), and (iii) Berry (12%).

With the exclusion of nickel entries, constituting the bulk of the TBPs in the data, factors associated primarily with with the SQP conformation, such as the addition/elimination coordinate, ought to come into prominence, with those associated with the TBP falling by the wayside. As it turns out the exclusion has indeed made the addition/elimination coordinate more important, with the S_N2 coordinate still prominent in the unrotated factors, though. Curiously, rotation interchanges the factors and eliminates the S_N2 coordinate, resulting in the pattern expected on the basis of the results from T-space. In this case, then, rotation yielded more meaningful results than did the unrotated factors.

Discussion

1. Summary of Chemical Results. Cluster analysis has shown that the molecular geometry of five-coordinate d^8 complexes is characterized by three archetypal conformations—the trigonal bipyramid, a flattened square pyramid, and an elevated square pyramid. Collectively, the data exhibit distortions of these conformations that can be described in terms of adherence to an S_N2, a Berry, an addition/elimination and a glue coordinate, as the results of factor analysis have demonstrated.

TBP. Essential structural features of the TBP include large variances in the axial bond lengths (r_1 and r_5) and the degree of elevation of the metal atom out of the equatorial plane, with a correspondingly large range in the axial–equatorial angles. On average, the axial bonds are longer than the equatorial ones. The geometries of the ML_5 fragments classified as TBP essentially map a coodinate that is reminiscent of the distortions of the TBP along a S_N2 reaction pathway: a lenghtening of one axial bond, a shortening of the other, and a concomitant umbrella type distortion of the angles between the equatorial ligands and the two axial ones. The second factor delineates a coordinate involving simultaneously the closure of the axial angle (θ_{15}) and an opening of one of the equatorial ones (θ_{24}), an intramolecular distortion which parallels that of the Berry coordinate. Moreover, it appears that the increase in θ_{24} is considerably more important in distorting the TBP toward the SQP than is θ_{15} or than are any changes in bond lengths. The third and least important factor of the three involves the simultaneous lenghtening of the axial bonds and a shortening of the equatorial ones or vice versa. We have called this the constant-amount-of-glue coordinate or simply the glue coordinate. It reveals that the bonding of, e.g., the axial bonds may only be increased at the expense of that of the equatorial bonds or vice versa.

Of the metals constituting the data set nickel exhibits the greatest preponderance of TBP conformations (approximately 40% of the nickel entries), with rhodium and iridium following (18% and 26%), while palladium and platinum appear to adopt this conformation only under exceptional circumstances (0 and 1 case, respectively).

fSQP. A large variance in the position of the apical ligand with respect to the residual ML_4 fragment characterizes the fSQP. In other words, both the length of the apical bond and the angles between it and the other bonds are highly variable. The average apical bond for compounds classified with this group is considerably longer (by 0.8 Å) than the basal bonds, and the average trans-basal angle lies at 171°. The data primarily cluster along a pathway that maps a combination of the glue coordinate—describing the simultaneous shortening of the apical and lengthening of the basal bonds or vice versa—with a coordinate describing the elevation or degree of pyramidalization of the fSQP. This combined coordinate is reminiscent of the distortions manifested by an ML_5 moiety constituted by the square planar ML_4 fragment and the fifth ligand, L, during a reversible addition/elimination reaction at a four-coordinate center. The glue component of the addition/elimination coordinate is far more important for fSQP than it was for the TBP; the relation between the apical bonding electron density and the basal one appears to be of a much greater sensitivity than that between the axial and the equatorial bonds. The data suggest, however, that at *large* distances the apical ligand does not influence the geometry around the metal in a very consistent way.

The Berry coordinate is not manifested by the fSQP data. Instead, it seems that—under the constraint of C_{4v} symmetry—the fSQP cannot undergo intramolecular exchange via the Berry mechanism unless a certain degree of pyramidalization has been achieved.

The tendency toward this conformation is greatest for palladium and platinum, the majority of whose complexes adopt it, with approximately half the square pyramidally disposed nickel complexes also conforming to it. Rhodium and iridium, on the other hand, do not appear in this cluster at all—their SQP complexes are all part of the eSQP cluster.

eSQP. This conformation is characterized by an apical bond length which is much nearer that of the basal bonds than was the case for the fSQP and whose variance relative to that of the basal bonds is also much reduced. The structure of this archetype is altogether less variable than that of the fSQP, and its average trans-basal angle is 163°. The distortion coordinates along which the members of this cluster lie map, first, the addition/elimination and, second, the Berry coordinate, the latter in contrast to the fSQP. As was the case for the TBP, this coordinate is dominated by changes in the angles, changes in bond lengths being negligible. The least important factor describes the flexibility in the apical ligand, which is reduced, though, over what it was in the fSQP.

The addition/elimination coordinate appears to differ slightly from that for the fSQP, in that changes in bond distances and the pyramidalization of the ML_5 fragment are almost equally important. This suggests that the addition of a fifth ligand to the ML_4 moiety may be accompanied by increasing elevation of the SQP, in contrast to the results obtained for the fSQP, which indicated a decreased dependency between these two components. Consequently, the approach of the fifth ligand to the ML_4 fragment seems initially to bring about only a small elevation of the SQP, which becomes increasingly enhanced, however, as the proximity of the apical ligand increases. As mentioned earlier, the tendency to adopt this conformation is greatest for rhodium and iridium and is much lower for palladium and platinum.

2. Reaction Coordinates of the ML_5 Fragment. Five-coordinate intermediates and/or transition states have been postulated and demonstrated for many ligand-exchange reactions of square-planar molecules. They have historically been divided into three main groups—nucleophilic substitutions, electrophilic substitutions, and oxidative additions followed by reductive eliminations. It is becoming increasingly clear, however, that a relationship exists between many types of reaction mechanisms previously classified quite separately.[12-14] Often this relationship appears to result from *geometrically similar* reaction pathways involving the formation of a five-coordinate species, be it a true intermediate in an associative nucleophilic substitution, an early transition state in an oxidative addition, or a solvento species in a dissociative electrophilic substitution, for example. In this sense, then, many if not most reactions of four-coordinate complexes can be deemed at some stage to involve the formation of a five-coordinate species via an essentially associative mechanism:

$$XML_3 + Y \rightleftharpoons [XML_3Y] \rightleftharpoons X + ML_3Y$$

where X and L represent any coordinated ligand atoms and Y is either X, L, or solvent. There is general agreement that this reaction involves attack (nucleophilic or electrophilic) at the metal by the incoming "ligand" Y, with the five-coordinate adduct adopting TBP and SQP conformations at various stages along the reaction pathway. In most cases, though, geometrical details concerning conformational changes along the reaction have not been forthcoming. Cross[12-14] has reviewed the published work in this area with particular attention to the geometrical implications of the studied reactions,[13] but most of his conclusions have had to remain speculative in this regard, due to the classic difficulty of direct observation of the reaction species.

In his review, Cross sketches the results of mechanistic and kinetic studies on nucleophilic substitutions of, mainly, square-planar platinum and palladium complexes, on the one hand, and oxidative additions to the compounds of iridium and rhodium, on the other. He points out that this apparent bias toward the two types of reactions for the different metals reflects the nature of the available data, though to some extent it possibly also reflects inherent differences between the two groups of metals. We shall outline the broad conclusions drawn by Cross, adding to these the data we have earlier compiled on the dynamic stereochemistry of five-coordinate nickel,[15] as well as relevant studies published since his review appeared.

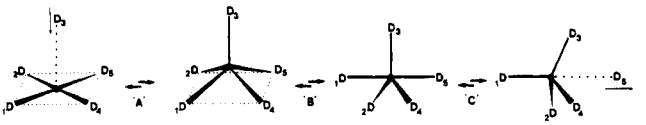

Figure 3. Diagram of essential reaction pathways of a five-coordinate fragment ML_5. A maps the reversible addition of a fifth ligand to a square-planar center, and the progression from a fSQP to a eSQP, B maps the SQP → TBP transformation according to the Berry coordinate, and C maps a reversible S_N2 reaction at a tetrahedral center.

Figure 3 outlines the essential reaction pathways followed by the pentacoordinate intermediate or transition state $[XML_3Y]$, as suggested by the mechanistic and kinetic data documented both by Cross for rhodium, iridium, platinum, and palladium and by us for nickel.[15] The addition of an incoming ligand is proposed to take place along the perpendicular to the ML_4 fragment, giving rise to a square-pyramidal species (step A), though a distinction is never made between a fSQP and an eSQP. It is further suggested that this species often distorts along the C_{2v} Berry coordinate into a TBP (step B), which may, in turn, distort toward yet another isometric SQP. In the case of nickel compounds, the dissociation of the TBP intermediate via an S_N2 coordinate has sometimes been indicated (step C). This pathway has also been involved in a few examples of nucleophilic substitutions and isomerization of tetrahedral nickel complexes.[15]

Until recently, it remained uncertain whether the five-coordinate species possesses sufficient stability to be regarded as an actual intermediate, rather than merely as a phase of the activated complex. However, on the basis of a mass spectrometric study of the addition of chloride ion to $[PtCl_2(PEt_3)_2]$, Turco et al.[16] have suggested the formation of a true five-coordinate adduct with a lifetime greater than 10^{-5} s. They leave open the question, though, of whether the intermediate they have found is in fact distinct from the transition state for the addition reaction or not.

Often more concrete evidence for the formation of five-coordinate intermediates appears to be inferable from studies of association reactions or ligand exchanges at four-coordinate complexes. The addition of cyanide ion to $[PtL_2]^{2+}$ (L = 1,10-phenanthroline or 2,2′-bipyridine), for example, gives rise to an isolable five-coordinate species $[PtL_2(CN)]^+$, which is also indicated as the intermediate in the reaction leading to $[PtL(CN)_2]$. Using these two examples, Wernberg[17,18] has also shown that the rate of ligand substitution leading to the product $[PtL(Nu)_2]$ for various nucleophiles (Nu) is faster in the case of the bipyridyl complexes than in that of the phenanthroline compounds. He has rationalized this in terms of the bipyridyl ligand being more flexible and consequently a better leaving group than phenanthroline. Quite likely, though, it is the lower rigidity of the bipyridine *in combination* with the nature of the five-coordinate complex that results in the enhanced kinetics; he has suggested that the phenanthroline-containing intermediate exhibits intramolecular exchange in accordance with the Berry mechanism.[19] These examples highlight the crucial role which the five-coordinate adduct often plays as a result of its particular geometric features.

The character of the intermediate has also been put forward as a factor in explaining kinetic data obtained for olefin exchange in a series of *trans*-dichloro(η-olefin)(pyridine)platinum(II) complexes with various substituents on pyridine. Chottard and

(12) Anderson, G. K.; Cross, R. J. *Acc. Chem. Res.* **1984**, *17*, 67–74.
(13) Cross, R. J. *Chem. Soc. Rev.* **1985**, *14*, 197–223.
(14) Cross, R. J. In *Mechanisms of Inorganic and Organometallic Reactions*, Plenum Press: New York, 1984; Vol. 2, Chapter 5.
(15) Auf der Heyde, T. P. E.; Nassimbeni, L. R. *Inorg. Chem.* **1984**, *23*, 4525–4532.
(16) Turco, A.; Morvillo, A.; Vettori, U.; Traldi, P. *Inorg. Chem.* **1985**, *24*, 1123–1125.
(17) Wernberg, O. *Acta Chem. Scand.* **1985**, *A39*, 223–225.
(18) Wernberg, O. *J. Chem. Soc., Dalton Trans.* **1986**, 725–728.
(19) Wernberg, O.; Hazell, A. *J. Chem. Soc., Dalton Trans.* **1980**, 973–978.

Guillot-Edelheit[20] describe how this exchange is catalyzed by the transient chelation of a hydroxy group on the pyridine resulting in the formation of a five-coordinate species.

Stereochemical nonrigidity and, in particular, intramolecular exchange via principally the Berry mechanism have been documented in a number of cases for nickel,[15] although evidence for this reaction in complexes of the other metals is scanty.[11-14,21] Where it has been suggested, it is often done simply on the basis of temperature-dependent NMR studies and not on the basis of unambiguous kinetic studies. Yamazaki, for example, suggests a fluxional palladium complex of a substituted phenanthroline on the basis of variable-temperature NMR experiments and describes its dynamic motion as an intramolecular rearrangement akin to the Berry mechanism.[22] A similar facile rearrangement between TBP and SQP conformers of a dicarbonyl bis(triphenylphosphine) complex of rhodium has been suggested, again on the basis of NMR studies.[23] Although in many cases the Berry mechanism has been invoked without sufficient experimental support, there nevertheless are examples in which it seems highly plausible.[13,15,21]

Finally, some tetrahedral nickel complexes have been demonstrated to undergo nucleophilic substitution of ligand exchange reactions involving the simultaneous attack and departure by two ligands in the same way as the classic S_N2 reaction at tetrahedral carbon has been conceptualized.[15]

Conclusion

Comparing the results of the statistical analysis with the mechanistic data that have been collected for the ML_5 fragment, it it difficult to avoid the conclusion that the static deformations manifested by the five-coordinate molecular fragments constituting our data set do indeed mirror those proposed to occur in solution for this fragment.[24] The mathematical techniques applied to the data have yielded correlations between independent geometrical parameters (the symmetry coordinates) that map molecular distortions identical with those proposed to occur along certain reaction pathways for the ML_5 molecular fragment. These results, then, call for an interpretation in terms of the structure correlation hypothesis: If a correlation can be found between two or more independent parameters describing the structure of a given structural fragment in a variety of environments, then the correlation function maps a minimum energy path in the corresponding parameter space.[25]

In some instances, this analysis has revealed trends that are perhaps implicit in available mechanistic data on the solution behavior of molecules containing the ML_5 moiety, although they have yet to be explicitly stated. For example, the metals studied here appear to fall into three categories.[26] The first, containing platinum and palladium, hardly adopts TBP conformation and prefers the fSQP over the eSQP. In contrast, the second grouping, consisting of rhodium and iridium, adopts TBP conformation in roughly one-fifth of the cases and prefers the eSQP, while the third, consisting of nickel, is intermediate between the two, having a slight preference for the eSQP over the TBP and fSQP. The difference between the chemistry of nickel and that of the other metals is already evident in the fact that its four-coordinate complexes can adopt either tetrahedral or square-planar conformation, while the latter only is exhibited by the others. This obviously has implications for the range of reaction pathways available to five-coordinate nickel, as the mapping of the S_N2 pathway by, predominantly, the nickel complexes shows. However, the presence—albeit a reduced one—of this distortion coordinate in the data even *after* the removal of the nickel compounds indicates that this pathway might also be available to rhodium and iridium (the other constituents of the TBP cluster), even though this may not be evident from the chemistry of their four-coordination.

Platinum and palladium complexes have been shown to preferentially adopt the fSQP conformation, which does not manifest the Berry distortion. As a result, one would expect only a few instances of intramolecular exchange via this mechanism for five-coordinate complexes of these metals. The scarcity of experimental data that unambiguously indicate this type of fluxionality for platinum and palladium may, consequently, indicate that other mechanisms are operable in most intramolecular exchange reactions of these metals. Rhodium and iridium, on the other hand, have a very clear preference for the eSQP, which does exhibit Berry distortions. This would suggest that the Berry coordinate represents a viable option for intramolecular exchange in these metals, in contrast to platinum and palladium.

We must stress, however, that these conclusions must be seen in the context of our choice to perform the analysis in D_{3h} and C_{4v} symmetry spaces throughout. This choice imposed constraints that may not have been present had we chosen C_{2v} symmetry instead. For example, the differentiation of square-pyramidally disposed conformations into eSQP and fSQP clusters may have been facilitated by this constraint, and our conclusions in this regard therefore need to be treated with caution.

Finally, in our experience, the techniques we have applied in this study have been very powerful in extracting information from the data set. There are two observations, however, that need to be made. The first concerns the automated nature of the analysis—this represents an obvious advantage in that results can be objectively and speedily obtained. It also carries with it, though, the danger of alienating the analyst from the data since the automatic routines and algorithms remove the necessity of "hands-on" work; the often invaluable intimate contact with the data can thereby be lost. The second point relates to the nature of the information derived from the analysis. A data set such as ours contains a veritable treasure trove of information, while the powerful techniques offer us tools with which to excavate the hoard. Obviously, among much useful information there will be masses of trivia, and inevitably the question arises: Where does one stop? The answer to this question is not at all simple. The possibility of refining the techniques so as to obtain more and more information, coupled to that of uncovering new secrets (however trivial they may be), represents a strong incentive to continuing the analysis almost ad infinitum (and ad absurdum).

(20) Guillot-Edelheit, G.; Chottard, J.-C. *J. Chem. Soc., Dalton Trans.* **1984**, 169-173.
(21) Deeming, A. J.; In *Mechanisms of Inorganic and Organometallic Reactions*; Plenum Press: New York, 1984; Vol. 2, Chapter 13.
(22) Yamazaki, S. *Bull. Chem. Soc. Jpn.* **1987**, *60*, 1155-1156.
(23) Sanger, A. R. *Can. J. Chem.* **1985**, *63*, 571-575.
(24) We must caution against an overly naive interpretation of this, though. For example, insofar as our data set contained no explicitly electrophilic ligands, it would be highly speculative to extrapolate these results to all substitution reactions of four-coordinate d^8 complexes.
(25) (a) Bürgi, H.-B. *Inorg. Chem.* **1973**, *12*, 2321-2325. (b) Murray-Rust, P.; Bürgi, H.-B.; Dunitz, J. D. *J. Am. Chem. Soc.* **1975**, *97*, 921-922.
(26) See Table VIII of ref 1.